# Aging and Characterization of Li-Ion Batteries in a HEV Application for Lifetime Estimation

**Pierfrancesco Spagnol*, Simona Onori*, Nullo Madella*, Yann Guezennec*,**, John Neal***

**Center for Automotive Research, The Ohio State University, Columbus, OH 43212 USA*
*(email: {spagnol.1;onori.1;madella.1;neal.166}@osu.edu )*
*** Department of Mechanical Engineering, The Ohio State University, Columbus, OH 43212 USA*
*(email: guezennec.1@osu.edu)*

**Abstract**: This paper deals with the aging and characterization of lithium-ion (Li-ion) batteries for life estimation evaluation. The most important aging characteristics of a real driving cycle for hybrid electric vehicle application, such as initial State of Charge (SoC) and Depth of Discharge (DoD), are used to synthesize an aging profile to be reproduced in laboratory based on statistical analysis. Implementing the synthesized driving cycle at higher temperature results in an accelerated aging. Periodic assessment tests are also performed within the aging activity in order to monitor the behavior of two battery aging parameters, namely, resistance and capacity. The evolution of these two parameters is monitored and a general framework for battery parameter estimation based on a predictor/corrector scheme is presented.

*Keywords:* P/HEV Battery, Automotive, Duty cycles, Signal processing, Test generation.

## 1. INTRODUCTION

Compared with lead-acid batteries and nickel-metal hydride (Ni-MH) batteries, Li-Ion technology based batteries are superior in terms of specific energy (the amount of available energy per unit of mass or volume) and specific power (the amount of available output per unit of mass or volume). As a result, they are seen as the most promising and suitable technology for electric vehicles (EV), hybrid electric vehicle (HEV) and plug-in hybrid electric vehicles (PHEV) applications and they are expected to replace NiMH batteries in HEVs within the next years [7].

Battery requirements differ by the specific application [1], [5]. High power is needed to provide adequate boost in HEV applications. Power density is less important in PHEV and EV applications due to their larger high-energy battery. On the other hand, as energy translates into vehicle range, high energy is needed to provide adequate mile range. This is more important for PHEVs and EVs than for HEVs. In fact, a HEV battery is operated in charge sustaining mode at intermediate SoC through shallow cycles and only uses a small part of the available energy. Thus, HEV batteries differ from PHEV and EV batteries, in that they require power rather than energy density.

The ability of these advanced batteries to maintain their power and energy characteristics for tens of thousands of miles is essential to ensure consumer acceptance of electrified powertrains. In the context of vehicle electrification, research and development of advanced energy storage systems, particularly advanced battery systems, play a major role. During driving operations, batteries are subject to several cycles of charge and discharge, which in some cases may occur in a relatively short time. Such usage patterns contribute to accelerating the battery aging process, decreasing the lifetime of battery pack/module/cell and increasing the cost of vehicles.

The objective of this paper is to describe how Li-Ion battery aging and characterization is perfomed in laboratory environment for HEV applications and how a life estimation framework can be designed. The life estimation method is very genearal and can be used and adapted to track both power fade and/or energy fade depending on the specific application considered (HEV, PHEV and EV).

Starting from data collected in vehicle and extracting useful stastistical characteristics of a real driving cycle, an aging profile has been synthetized to be run in laboratory (Section 2 and 3). Using the sythesized cycle will result in an easy implementable and repeatable aging cycle shorter than the real one. The experimental activity is composed of aging cycles spaced out by periodic assessment tests, where a "snapshot" of the battery is taken in terms of its ongoing aging parameters. The battery resistance and capacity are the two aging parameters defining the battery performance in terms of available power and available energy. Monitoring the evolution of the battery capacity and resistance during aging is crucial for the design of a lifetime estimation algorithm. In Section 4 the test plan developed for battery aging is discussed and in Section 5 the analysis of the aging data is presented. Section 6 discusses the overall framework for aging paramter estimation. Future work and conclusions are presented in Section 7 an 8.

## 2. SYNTESIZED DUTY CYCLE

Battery aging depends on the way it is used [3] and, in general, is a function of

- Current Magnitude;
- Temperature;
- Operating SoC/DoD.

Higher temperatures age the battery faster than lower temperatures; discharging a battery starting from a low initial SoC and/or high DoD speeds up the aging process as well. High magnitude currents also contribute to a faster aging.

All this information is intrinsically embedded into the real current that goes into and comes out of the battery. From a practical point of view, real driving cycles are not used to age the batteries in a laboratory setup, but rather an *ad hoc* synthetic aging profile best fits within a laboratory study.

A synthesized (simplified) current profile is designed from real data which maintains the same statistical characteristics of the real profile. The aging current profile must be representative of the main aging factors the battery is subject to during its normal operation, so initial SoC and DoD of the real driving cycle are reflected within the synthesized cycle. The aging protocol developed has been implemented in our battery aging facility, which consists of 12 battery cyclers operating on a 24/7 basis, complete with Peltier junctions to control the thermal environment.

The procedure described below can be applied to every data set which is statistically representative of actual vehicle operation (real-world driving cycle). The convention used is: positive currents correspond to charge and negative current to discharge.

### *2.1 Analysis of real current profile*

The real current profile I [A] acquired during a typical HEV driving operation is normalized with respect to the battery pack nominal capacity $S_c$ [Ah], according to:

$$C_{rate} = \frac{I}{S_c} \quad (1)$$

The current profile expressed in terms of C-rate is shown in Fig. 1. For typical HEV applications the battery $C_{rate}$ normally stays approximately within a range of [±10C]. The current profile in terms of C-rate, ranging between –6C to 10C, is then "discretized" into 2-C length bin as shown Table 1. The number of bins was chosen to be as small as possible but at the same time to capture the main aging effects on the battery. The histogram of the battery current distribution in terms of C-rate is shown in Fig. 2.

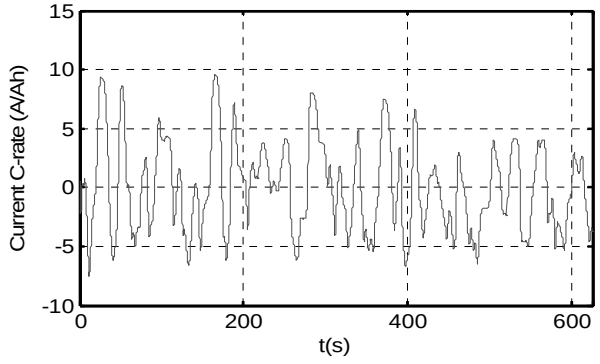


Fig. 1 Cell level current profile for a HEV during an actual driving cycle, expressed in terms of C-rate

Table 1. Current C-rate bins

| Bins | Current C-rate range |
|---|---|
| -6C | [-7C, -5C] |
| -4C | [-5C, -3C] |
| -2C | [-3C, -1C] |
| 0C | [1C, -1C] |
| 2C | [1C, 3C] |
| 4C | [3C, 5C] |
| 6C | [5C, 7C] |
| 8C | [7C, 9C] |
| 10C | [9C, 11C] |

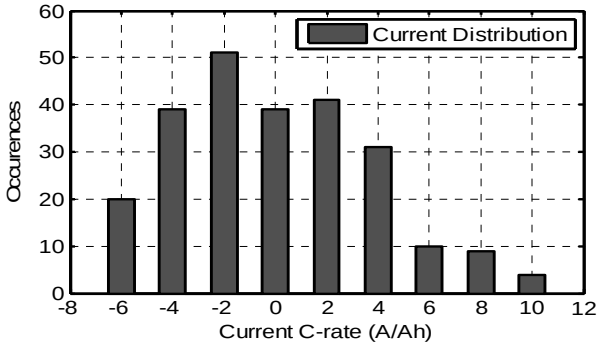


Fig. 2 Current distribution histogram of the real driving cycle and synthesized one

### *2.2 Engineer the duty cycle*

In the process of engineering the aging current profile for a HEV application, the main objective is to keep the same statistical distribution of the current C-rate and DoD, at known initial SoC. This guarantees that the duty cycle implemented in laboratory mimics the real one, in what exhibits main features of the real data set.

Thus, the synthesized current profile turns out to be:

- shorter than the real one;
- easy to implement;
- repeatable.

As a result, the heuristic design based on statistical distribution approach produces the cycle shown in Fig. 3. The histogram of both the synthesized current profile is the same as the one of the real driving cycle, depicted in Fig. 2. The DoD of the real driving cycle, shown in Fig. 4, has been fairly replicated in the synthesized profile as shown in Fig. 5.

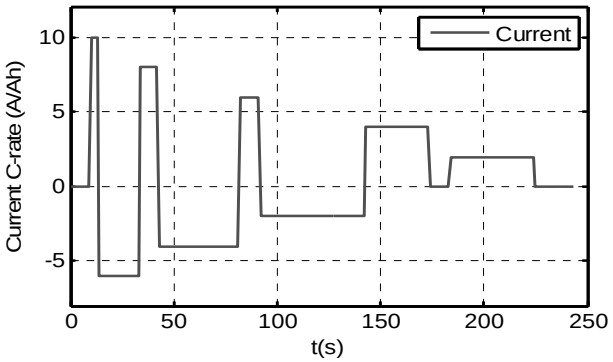


Fig. 3 Synthesized current profile

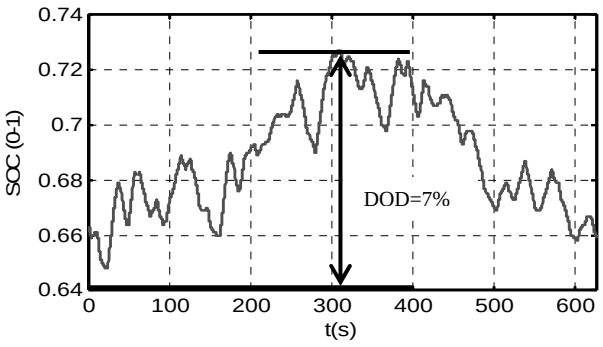


Fig. 4 SoC profile and DoD of the real driving cycle

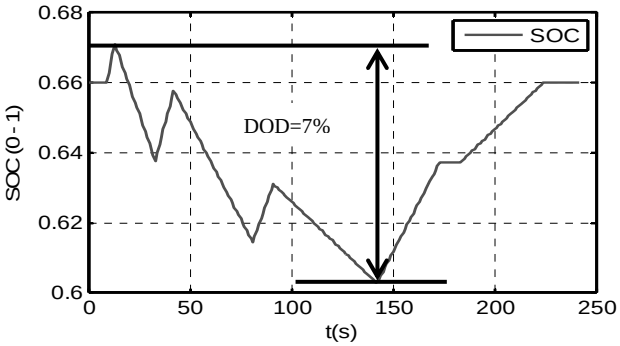


Fig. 5 SoC profile and DoD of the synthesized driving cycle

## 3. EXPERIMENTAL SETUP

The aging experiments were carried out in the battery characterization and aging laboratories at the Center for Automotive Research of The Ohio State University.

The laboratory contains multiple stations capable of running tests of arbitrary lengths. Each testing station is based on a pair of programmable load and power supply, a data acquisition device and control computer, Peltier junctions and associated controllers to provide a controlled thermal environment for the battery under test for temperatures ranging between -25 °C and 60°C. Each experimental station consists of a 1.5kW programmable electronic load and a 3.3kW programmable power supply.

The battery voltage is measured at the terminals of the battery at a sampling rate of 10 Hz. For the experiments described in this paper, all the aging tests were conducted at an isothermal temperature of 45 °C via Peltier junctions, while the assessment tests were performed at 25 °C.

The synthesized aging profile is repeated continuously and automatically on the aging station while data are acquired.

The battery under testing is an A123 System lithium ion rechargeable ANR26650 cell. It is a phosphate-based system with nominal voltage of about 3.3V/cell, peak charge voltage of 3.60V and nominal capacity of 2.3Ah. In this paper, experimental results of three cells are discussed and analyzed.

## 4. AGING AND CHARACTERIZATION ACTIVITY

The aging and characterization activity consists of feeding the battery with a series of aging profiles (Fig. 3) space out with regular assessment tests to monitor the variation and degradation of battery parameters during aging. Moreover, an initial assessment test is done to evaluate the aging parameters at the beginning of battery life. The aging activity is then performed, followed by periodic assessments. The aging temperature is 45°C, while the assessment temperature is 25°C. The assessment tests, performed at 100% SoC are:

- Capacity test at C/1 rate, [3];
- Pulse Power test , [3];
- Cold Start Test at -20°C, [3];
- Resistance measurement with milliohm meter;
- Electrochemical Impedance Spectroscopy (EIS) test [8].

The aging campaign between any two assessments consists of 13 sets of aging, each of them of 300 synthesized aging cycles, for a total of 3900 cycles for each campaign.

An aging cycle corresponds to one tenth of a fully charge and fully discharge cycle, in terms of Ah extracted, as shown in Table 2.

Table 2. Equivalence between aging cycle and fully charge and discharge cycle

| Aging cycle | Ah-throughput at cycle | Corresponding fully charge and discharge cycle |
|---|---|---|
| 1 | 0.48 Amph | ~0.1 |

## 5. DATA ANALYSIS

In this work the capacity (related to energy fade) and resistance (related to power fade) measurements are considered as they change along the aging. In Fig. 6, the capacity of three batteries aged following the protocol previously described is plotted versus the total Ah throughput showing a decreasing trend. A 15% capacity variation with respect to its nominal value is reached after almost 11000 Ah were taken out and put into Battery 1 and roughly 23000 cycles were performed. Battery 2 had a shorter life, due to a laboratory instrumentation issue. However the capacity trend is still the same as the one of Battery 1. As far as Battery 3 goes more capacity tests were performed during the aging (basically a quick capacity test performed every 6 sets of aging) to have more data points to track the evolution of the capacity in case of instrumentation failures (as happened to Battery 2). Battery 3 showed a different capacity degradation trend compared to Battery 1 and Battery 2, although the aging conditions (temperature, current profile and initial SOC) were the same. This phenomenon can be explained as due to the variability of aging degradation mechanisms within the same type of battery cells showing that not all batteries behave the same. The importance of monitoring the capacity degradation is in the ability of possibly tracking the energy fade occurring

during vehicle operation, especially in PHEV and EV application. Note that, capacity can only be assessed in laboratory though.

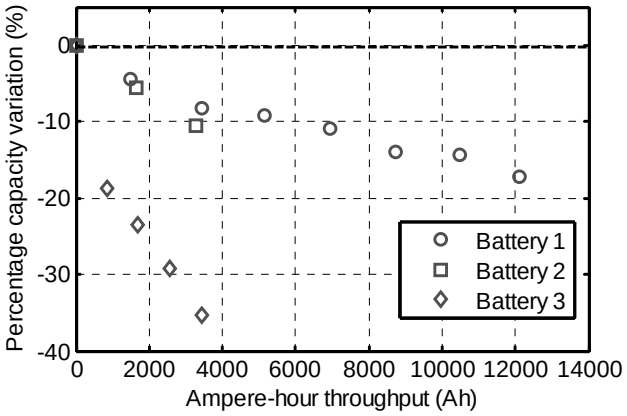


Fig. 6 Percentage variation of capacity with respect to its nominal value

On the other hand, for HEV application the power capability is of interest. Monitoring the resistance increase during aging would allow tracking power fade during vehicle operation. Considering the testing protocols described in [3] it is possible to define a way for monitoring the power fade at a given SoC as:

$$P_{discharge}(SoC) = \frac{V_{min}(V_{OCV}(SoC)-V_{min})}{R_{discharge}(SOC)} \quad (3)$$

$$P_{charge}(SoC) = \frac{V_{max}(V_{max}-V_{OCV}(SoC))}{R_{charge}(SOC)} \quad (4)$$

where:

$P_{discharge}(SoC)$ and $P_{charge}(SoC)$ are the available powers of the cell in charge and discharge at a given SoC.

$V_{max}$ and $V_{min}$ are the recommended pulse charge and discharge cut-off voltages defined by the manufacturer, which are 3.8V and 1.6 V, respectively.

$V_{OCV}(SoC)$ is the open circuit voltage at a given SoC. This data can be found from manufacturer characterization graphs.

$R_{discharge}(SoC)$ and $R_{charge}(SoC)$ are the resistances evaluated in charge and in discharge at a specific SoC. These two quantities vary during the aging. The greater the resistance during aging the smaller the available power.

The SoC of operation is 70%, as discussed in Section II.

An assessment of the battery resistance can be performed both during the aging activity and the assessment tests. If some kind of correlation between on-board measurable parameters and off-board measurable parameters is found, then the available power evolution can be indirectly monitored through some of the on-board estimated variables.

During aging, we can evaluate an "equivalent" resistance using current and voltage profiles. With reference to Fig. 7 and Fig. 8 the quantity

$$R_{ch/disch,i} = \frac{V_{max,i}-V_{min,i}}{I_{max,i}-I_{min,i}} \quad (5)$$

is evaluated at each pulse both in charge and discharge.

The subscript *i* indicates the pulse *i* on the aging cycle. $V_{max,i}$ is the value of voltage when the current assumes the value $I_{max,i}$.

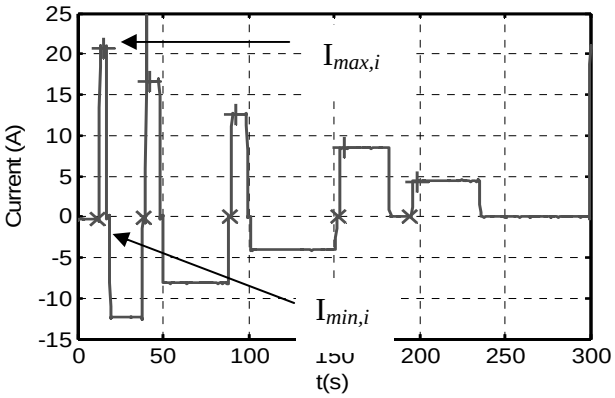


Fig. 7 Current profile used to calculate the equivalent resistance during charge

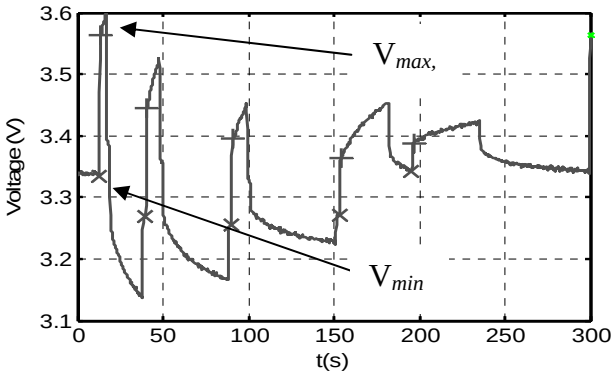


Fig. 8 Voltage response used to calculate the equivalent resistance during charge

In order to reduce the measurement noise, at each aging cycle (characterized by 5 charging pulses and 3 discharging pulses) the average of the charge resistance and discharge resistance is taken according to:

$$\bar{R}_{ch,j} = \frac{\sum_{i=1}^{5} R_{ch,i}}{5}; \quad \bar{R}_{disch,j} = \frac{\sum_{i=1}^{3} R_{disch,i}}{3} \quad (6)$$

Again, along an aging set (300 cycles) then average of the charge and discharge resistance along the aging set is considered:

$$\bar{\bar{R}}_{ch} = \frac{\sum_{j=1}^{300} \bar{R}_{ch,j}}{300}; \quad \bar{\bar{R}}_{disch} = \frac{\sum_{j=1}^{300} \bar{R}_{disch,j}}{300} \quad (7)$$

In the percentage variation of the "equivalent" resistance in charge compared to its initial value is shown. The same behavior is obtained for the discharge resistance.

Each data point of the aging data curve in Fig. 9 corresponds to an estimated $\bar{\bar{R}}_{ch}$, evaluated according to Eq. (7).

During the assessment tests instead, the value of the resistance of the battery is obtained using both the milliohm meter and EIS test. The squared data points in Fig. 9 show the trend of the resistance measured during the assessments. As one can see, the trend of the resistance (computed in two different ways) is very similar, i.e. increasing almost linearly with the aging.

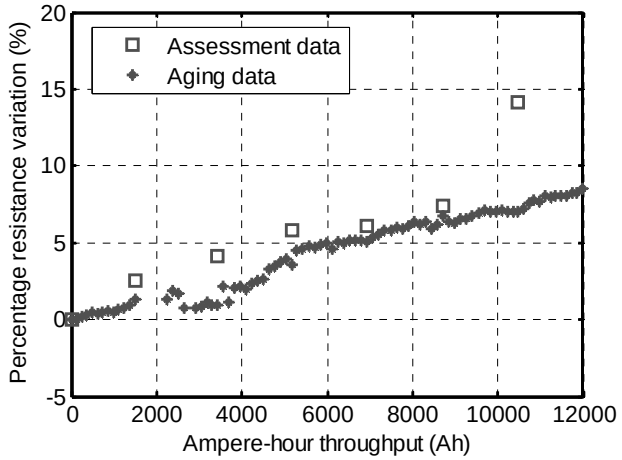


Fig. 9 Percentage variation of evaluated charge resistance (aging data) and measured resistance (assessment data) with respect to its initial value Battery 1

Evaluating the resistance during normal operations results in

i) richer data set (on-board computation allows having a *quasi*-continuous monitoring of the resistance during aging), and

ii) possibility to exploit methods for on-board implementation.

A comparison between the three batteries shows similar degradation behavior for Battery 1 and Battery 2, while Battery 3 experienced a severe decrease in performances at the same level of Ah throughput. All the three batteries show a linear behavior.

A correlation between the capacity decrease and resistance increase is shown in Fig. 10, where the capacity is measured during assessment tests whereas the resistance is evaluated from the aging at the same Ah throughput.

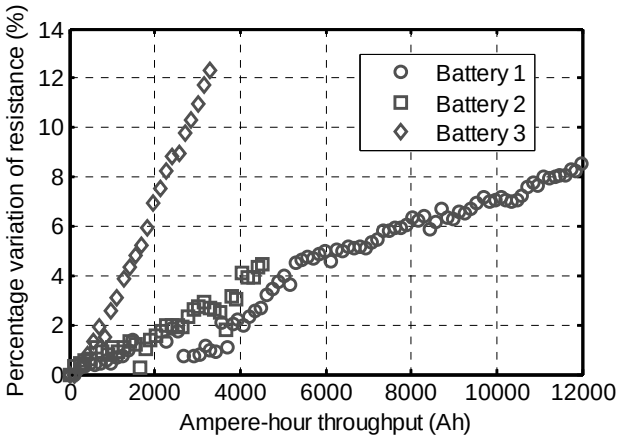


Fig. 1 - Percentage variation of evaluated charge resistance (aging data) for three different batteries with respect to its initial value

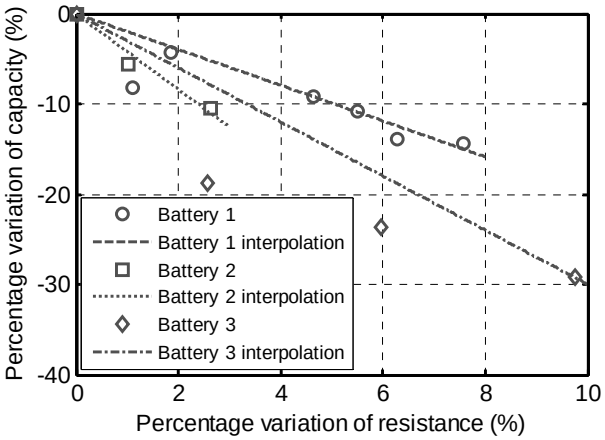


Fig. 10 Correlation between capacity and charge resistance

From the data points collected it is possible to assess that a correlation between the two aging parameters exists. However, due to intrinsic differences among the same type of batteries, a cone of uncertainty can be identified in Fig. 10 within which the degradation occurs. Further investigations based on more aging data would help to give some insight on this phenomenon.

## 6. GENERAL FRAMEWORK FOR PARAMETER ESTIMATION

The trend of the aging parameters recorded during the experiments on several batteries of the same typology and the measurement post-processed on a particular battery can be combined in a predictor/corrector scheme for parameter estimation as shown in Fig. 11. In this general framework, the predictor path exploits an aging model of one (or more) aging parameter, initialized starting from the historical data collected during past experiments (for a specific application), based on in-situ measurements of current, voltage and temperature.

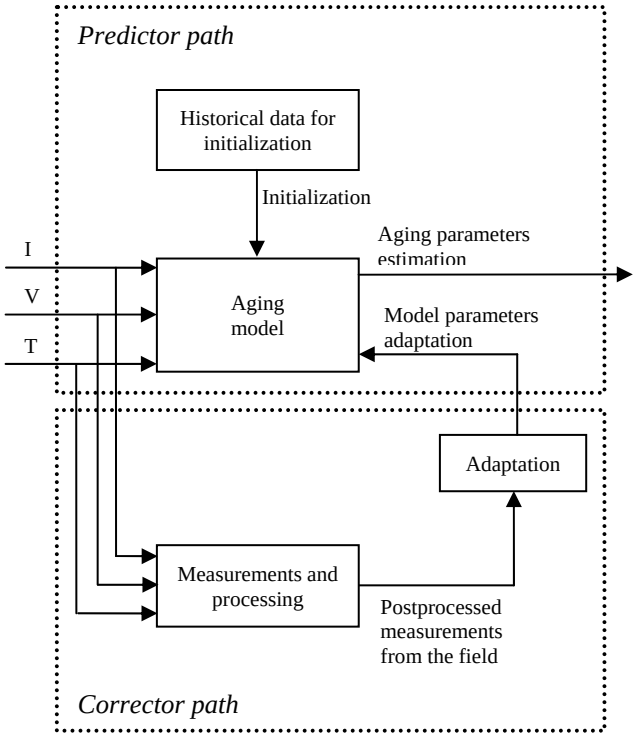


Fig. 11 General framework for aging parameter estimation

The predictor path needs to be updated due to the variability among same types of the batteries or/and slight different aging conditions that can change the normal degradation behavior of the parameter considered. Thus a corrector path is added to monitor the behavior of the degradation parameter and adapt and update the aging model accordingly.
This framework can lead to a robust estimation of battery life as:

- The corrector path is capable of adapting the aging model considering the variability associated to cell of the same type;
- The corrector path can correct the prediction model in presence of a battery with unknown history;
- The predictor path can work in presence of temporary sensor failures or corrupted measurements (corrector path unavailable);
- The predictor path can be used to predict the future behavior of the batteries considering past historical data and past measurement performed

## 7. FUTURE WORK

The data analysis showed and the general framework for aging parameter estimation can lead to the design of battery lifetime estimation algorithm, potentially implementable on-board. As the aging is continued and more data become available, the design of the battery life estimation algorithm can be carried out.

## 8. CONCLUSIONS

In this paper, a synthetic duty cycle profile has been engineered from a real driving cycle for HEV application for the purpose of performing aging and characterization activity. Data collected during aging and assessments showed a battery capacity decreasing and a resistance increasing trend. However, due to variability among the same typology of battery, the aging parameters behavior of three aged batteries shows different path, although the aging conditions were the same. Moreover, a general predictor/corrector framework for estimation of aging parameters is presented: this framework is based on on-board measurements that adjust the aging model initialized using historical data. This framework can be used not only for life estimation but also for battery prognosis.

## ACKNOWLEDGMENTS

The authors would like to thank the US Army - TARDEC (Tank and Automotive Research, Development and Engineering Center) for its financial support under which the majority of the work presented here was conducted. The findings and conclusions presented in this paper solely reflect the authors' research and do not constitute an official endorsement by the US Army – TARDEC.

## REFERENCES

1. F. Nemry, G. Leduc, A. Muñoz, *"Plug-in Hybrid and Battery-Electric Vehicles: State of the research and development and comparative analysis of energy and cost efficiency"*, JRC 54699 Technical note, 2009.

2. P. Spagnol, S. Onori, V. Marano, Y. Guezennec, G. Rizzoni , "*A life estimation method for Lithium-ion batteries in Plug-in Hybrid Electric Vehicles applications*" submitted for publication, International Journal of Power Electronics, Special Issue, May 2010.

3. *"FreedomCAR Battery Test Manual for Power-Assist Hybrid Electric Vehicles"*, DOE/ID-11069, October 2003.

4. Z. Chehab, L. Serrao, Y. Guezennec, and G. Rizzoni, "*Aging characterization of nickel metal hydride batteries using electrochemical impedance spectroscopy"*, *ASME* International Mechanical Engineering Congress and Exhibition, Chicago, November 2006.

5. D. Anderson, *Status and Trends in the HEV/PHEV/EV Battery Industry*. Rocky Mountain Institute, Summer 2008.

6. High Power Lithium Ion ANR26650M1A – Datasheet A123. www.a123systems.com

7. A. Pesaran,T. Markel, H. Tataria, D. Howell *Battery Requirements for Plug-In Hybrid Electric Vehicles – Analysis and Rationale*, 23rd International Electric Vehicle Symposium (EVS-23) Anaheim, California, December 2-5, 2007, NREL/CP-540-42240.

8. E. Barsoukov, J. R. Macdonald "*Impedance Spectroscopy- Theory, Experiments, and Applications*", 2nd Edition, Wiley, 2005.